



## INTERFACE BETWEEN CEMENT PASTE AND QUARTZ SAND IN ALKALI-ACTIVATED SLAG MORTARS

C. Shi<sup>1\*</sup> and P. Xie<sup>2†</sup>

\*Water Technology International Corporation, Operator of the Wastewater Technology Centre and the Canadian Clean Technology Centre, P.O. Box 5068, 867 Lakeshore Road, Burlington, Ontario, Canada L7R 4L7

†Department of Civil Engineering, University of Ottawa, Ottawa, Ontario, Canada K2N 6N5

(Received February 4, 1997; in final form March 30, 1998)

### ABSTRACT

Electrical conductivity measurement and scanning electron microscope (SEM) were used to examine the interfacial zone between cement paste and quartz sands in  $\text{Na}_2\text{SiO}_3$ -activated slag mortars.  $\text{Na}_2\text{SiO}_3$ -activated slag mortars exhibited a positive interfacial excess conductance, or a higher electrical conductivity of the interfacial zone between cement paste and quartz sands than that of bulk pastes. SEM observation indicated that no porous transition zone could be observed in  $\text{Na}_2\text{SiO}_3$ -activated slag mortar, but was found in Portland cement mortar. Because electrical conductivity depends on the pore structure and pore solution chemistry as well, it is speculated, based on published results, that the positive interfacial excess conductance was due to the high alkali concentration rather than a more porous structure around aggregate. Finally, a hypothesis on the formation of dense interface in  $\text{Na}_2\text{SiO}_3$ -activated slag mortars was advanced. © 1998 Elsevier Science Ltd

### Introduction

The interfacial zone between Portland cement paste and aggregate or reinforcement, which is characterized by the prevalence of calcium hydroxide and the higher porosity, is the weakest region that controls many important properties of concrete such as strength, permeability, and durability (1). The thickness of the transition zone, as determined by measurement of the orientation of  $\text{Ca}(\text{OH})_2$  crystal or microhardness, ranges from 50 to 100  $\mu\text{m}$  (2–3). To enhance the properties of concrete, attempts have been made to improve the interfacial zone (4–7). These methods can be divided into two classes: 1) coating aggregate surface with a low w/c paste, chemical reagents or polymers before mixing; and 2) partially replacing Portland cement with supplementary cementing materials such as silica fume, fly

<sup>1</sup>To whom correspondence should be addressed.

<sup>2</sup>Present address: Holderbank Engineering Canada Ltd., 2310 Lakeshore Road West, Mississauga, Ontario, L5J 1K2 Canada.

TABLE 1  
Chemical composition (mass %) and physical properties of BFS and PC.

Item	SiO <sub>2</sub>	Al <sub>2</sub> O <sub>3</sub>	Fe <sub>2</sub> O <sub>3</sub>	CaO	MgO	SO <sub>3</sub>	Na <sub>2</sub> O
BFS	35.33	9.94	0.62	34.65	14.63	3.97	0.31
PC	20.68	3.68	2.95	62.93	4.21	2.62	0.14

ash, and blast furnace slag. These methods usually complicate concrete mixing process. Also, the effectiveness for the enhancement of bond strength by these methods is still in dispute (4).

It is generally accepted that alkali-activated slag cement, which consists of ground granulated slag and an alkaline activator(s), may exhibit higher strength, denser microstructure, and better overall durability than Portland cement (8–9). The dense transition zone between cement paste and aggregate has been regarded as one of the main contributions to the better properties of alkali-activated slag concrete. Few studies have investigated the transition zone in alkali-activated slag concrete through the measurement of microhardness, and have found that the transition zone is harder than the bulk paste regardless of the nature of aggregate (10–11).

Several techniques, such as scanning electron microscopy, X-ray diffraction, and microhardness are often used to investigate the interface between cement paste and aggregate. Recently, an electrical conductivity method has been successfully developed for characterizing features of microstructure and formation process in the transition zone in Portland cement concrete (12–15). In this study, the electrical conductivity method, together with scanning electron microscopy, was used to examine the transition zone in Na<sub>2</sub>SiO<sub>3</sub>-activated slag mortar.

## Experimentation

### Raw Materials

A pelletized blast furnace slag (BFS) was used in this study. The characteristics of the BFS are given in Table 1. An X-ray diffraction analysis indicated that this slag consists mainly of glassy phase except for trace crystalline merwinite (3CaO·MgO·2SiO<sub>2</sub>). A previous study has indicated that Na<sub>2</sub>SiO<sub>3</sub>-activated slag mortars show a higher strength and a denser structure than a typical commercial ASTM (American Society For Testing and Materials) Type III Portland cement mortars at both early and later ages (16). A typical commercial ASTM Type III Portland cement was used in this study as a reference cement for the comparison of hydration products and the transition zone between cement paste and quartz. The chemical composition and some physical properties of the Portland cement are also given in Table 1.

Reagent grade Na<sub>2</sub>SiO<sub>3</sub>·9H<sub>2</sub>O was used as an alkaline activator. The activator dosage was 3% Na<sub>2</sub>O based on the mass of slag. Na<sub>2</sub>SiO<sub>3</sub>·9H<sub>2</sub>O was dissolved in mixing water first and then mixed with the slag and/or sand.

TABLE 1  
(Continued)

K <sub>2</sub> O	LOI	Total	Density (kg/m <sup>3</sup> )	Blaine Fineness (m <sup>2</sup> /kg)
0.44	0	99.89	2920	340
0.59	0.27	98.36	3140	495

### Preparation of Samples

Mortars for electrical conductivity measurement were prepared following ASTM C109 but with volumetric fractions of the standard Ottawa sands from 0 to 0.54. A constant water to slag ratio of 0.30 was used. The fresh mortars were cast in  $8.0 \times 8.0 \times 3.0$  cm cells and then cured in a fog room at temperature  $23 \pm 1^\circ\text{C}$ . Some cement paste without sand was also cast in small plastic vials for powder X-ray diffraction analysis of hydration products.

### Electrical Conductivity Measurement and Interfacial Excess Conductance

The electrical conductivity of concrete specimen  $\sigma(t)$  at hydration time  $t$  can be expressed as follows (13):

$$\left. \begin{aligned} \sigma(t) &= k(t)\varphi_a + b(t) \\ k(t) &= 3\left(\frac{\delta}{r}\right)\left(1 + \frac{\delta}{2r}\right)[\sigma_f(t) - \sigma_p(t)] - \frac{3}{2}\sigma_p(t) \\ b(t) &= \sigma_p(t) \end{aligned} \right\} \quad (1)$$

where  $\varphi_a$  is the volumetric fraction of aggregate in concrete;  $\delta$  is the thickness of the interfacial zone between cement paste and aggregate;  $r$  is the average radius of aggregate;  $\sigma_f(t)$  is the conductivity of the interfacial zone between cement paste and aggregate at time  $t$ ; and  $\sigma_p(t)$  is the conductivity of cement paste at time  $t$ .

A parameter  $\theta$ , referred as an interfacial excess conductance, is defined as:

$$\theta = \delta(\sigma_f - \sigma_p) \quad (2)$$

The following expression for  $\theta$  can be readily derived from Eq. 1:

$$\theta(t) = \delta[\sigma_f(t) - \sigma_p(t)] = r\left[\frac{k(t)}{3} + \frac{b(t)}{2}\right] \quad (3)$$

The slope  $k(t)$  and intercept  $b(t)$  can be readily obtained from the straight lines of  $\sigma(t)$  vs.  $\varphi_a$  using experimental results;  $\theta$  can be calculated using Eq. 3.

The resistance of mortars was measured at 1 to 35 days, then converted to electrical conductivity. Because the interfacial zone in Portland cement mortar has been extensively examined (12–15), only alkali-activated slag mortars were investigated in this study. The

apparatus for determining the resistance of mortar was described in a previous work (14). The electrical conductivity of mortars was calculated as follows:

$$\sigma = \frac{L}{S} \frac{1}{R} \tag{4}$$

where  $L/S$  is referred to as the cell constant (obtained by calibration with 0.1 N KCl solution).

**Powder X-Ray Diffraction (XRD) Analysis**

Powder XRD analysis was performed on ground alkali-activated slag and Portland cement pastes with a Philips PW 1139 Diffractometer. The phases were identified from the characteristic peak data base of the Powder Diffraction File of the Joint Committee on Powder Diffraction Standards.

**Scanning Electron Microscope (SEM) Observation**

Alkali-activated and Portland cement mortars were cut into small fragments with an axe and then placed in a bath of dry pentane cooled to about  $-125^{\circ}\text{C}$ . After 2–3 min. in the bath, these fragments were carefully moved to a vacuum freeze-drying apparatus for 24 h to remove all free water (16). These fragments were stored in sealed containers for SEM observation.

The interfacial zone between paste and quartz was examined under a Cambridge Stereoscan 150 Scanning Electron Microscope. Micrographs were taken of representative areas

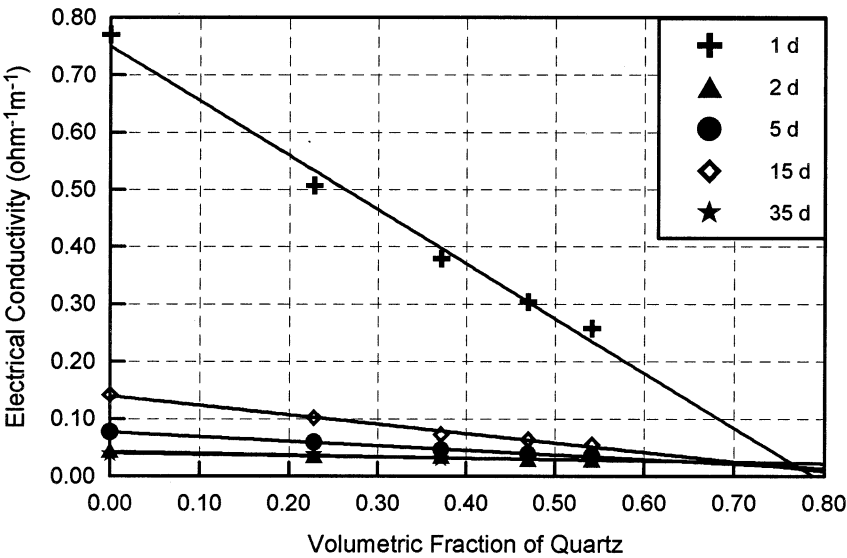


FIG. 1. Electrical conductivity of alkali-activated slag mortar vs. volumetric fraction of quartz sand.

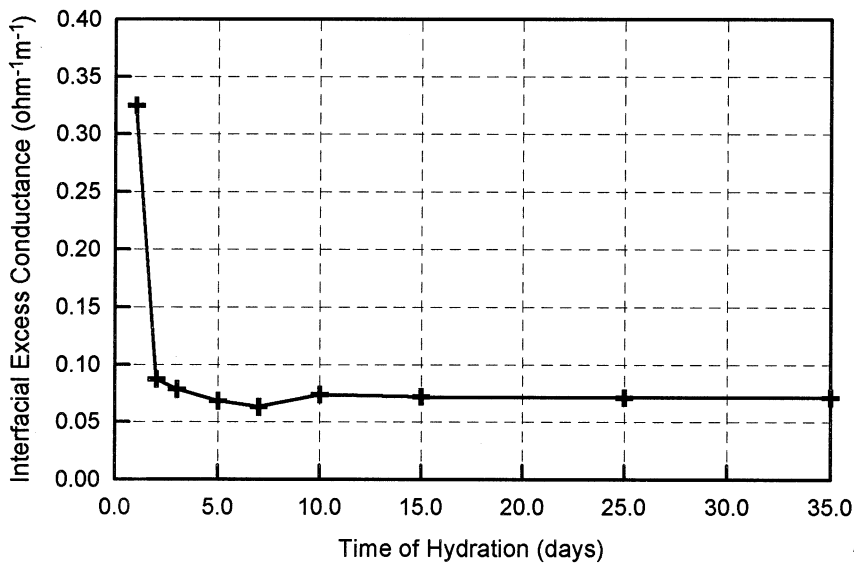


FIG. 2.  
Interfacial excess conductance of alkali-activated slag mortar.

at magnifications ranging from  $20\times$  to  $100,000\times$  after the interfacial zone of the sample was extensively viewed.

## Experimental Results

### Electrical Conductivity Measurement and Interfacial Excess Conductance

A plot of the electrical conductivity of the specimen vs. the fractional volume of quartz is shown in Figure 1. The straight lines were predicated by Eq. 1. The correlation coefficients for these fitted straight lines were greater than 0.98. This means that Eq. 1 can describe this type of cementing materials well. The effect of quartz fraction on the electrical conductivity of mortars decreased with time significantly during the first 2 days, and kept almost constant after 15 days. Thus, the hydration and structure formation of alkali-activated slag take place mainly during the first 2 days.

The interfacial excess conductance, which was obtained based on the slopes and intercepts of fitted straight lines in Figure 1 (some data were not plotted in Fig. 1), is plotted vs. hydration time in Figure 2. The interfacial excess conductance decreased quickly from 1 to 2 days and kept almost constant thereafter. This indicates that the structure formation of transition zone is almost completed during the first 2 days of hydration. This is in agreement with the findings from Portland cement mortars (13). The positive value of the interfacial excess conductance means that the conductivity of transition zone between cement paste and quartz is greater than that of the bulk pastes in alkali-activated slag mortars.

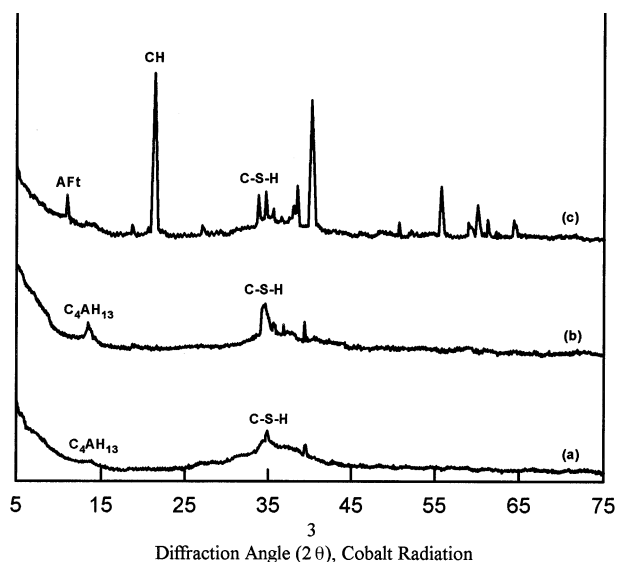


FIG. 3.

XRD patterns of  $\text{Na}_2\text{SiO}_3$ -activated slag and Portland cement pastes. (a)  $\text{Na}_2\text{SiO}_3$ -activated slag after 1 day of hydration; (b)  $\text{Na}_2\text{SiO}_3$ -activated slag after 540 days of hydration; (c) Portland cement after 540 days of hydration.

### Powder X-Ray Diffraction Analysis of Hydration Product

To better understand the microstructure of the transition in alkali-activated slag and Portland cement mortars, powder XRD analysis was carried out to identify the hydration products in alkali-activated slag and Portland cement pastes, as shown in Figure 3. The XRD patterns of Portland cement at 1 and 540 days were essentially the same, except for some differences in intensity. Only the pattern at 1 day is presented. The detected hydration products in hydrated Portland cement are C-S-H,  $\text{Ca}(\text{OH})_2$ , and ettringite (Aft). The C-S-H in hydrated Portland cement has a C/S ratio of approximately 3 at early ages and 1.5 at later ages (17). C-S-H is the major phase and  $\text{C}_4\text{AH}_{13}$  is the trace phase in  $\text{Na}_2\text{SiO}_3$ -activated slag pastes. One study has found that the C/S ratio of C-S-H in activated slag paste ranged from 0.66 to 0.91 (18) and another one found it ranging from 0.9 to 1.2 (10).

### Scanning Electron Microscope Observation of Transition Zone

A typical microstructure of the interfacial zone between the cement paste and quartz sand in Portland cement mortars is shown in Figure 4. A thin layer of products, which is regarded as the duplex film, adhered on the surface of the sand grain. Beyond it, there was a porous transition zone with a thickness of 40 to 60  $\mu\text{m}$ . A high density of  $\text{Ca}(\text{OH})_2$  cluster could be observed in the porous transition zone. No crystalline morphology, as would be expected of Aft, was observed although it was detected in powder X-ray diffraction test. As age proceeded, the porous transition zone became thinner and denser.

In contrast with Portland cement mortar, significantly fewer exposed sand grains were

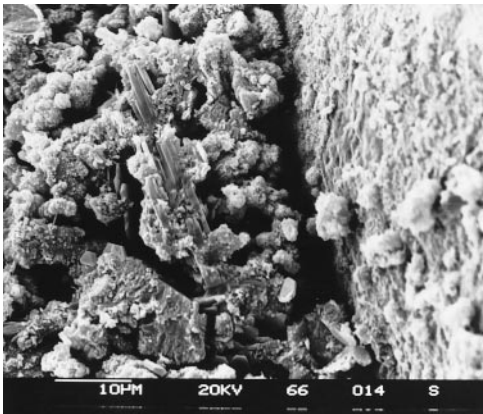


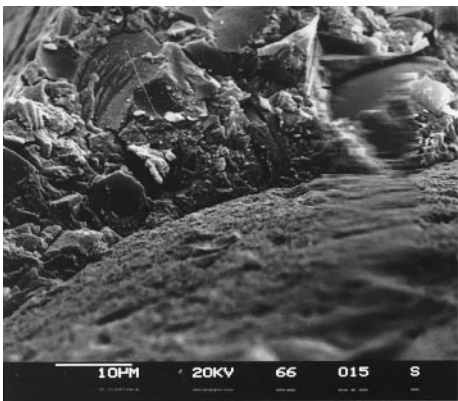
FIG. 4.  
Transition zone between type III Portland cement paste and quartz.

observed on the fracture surface of alkali-activated slag mortars. Figure 5 shows the typical microstructure observation of the interfacial area in alkali-activated slag mortars. The interfacial area appeared to be very dense and uniform.

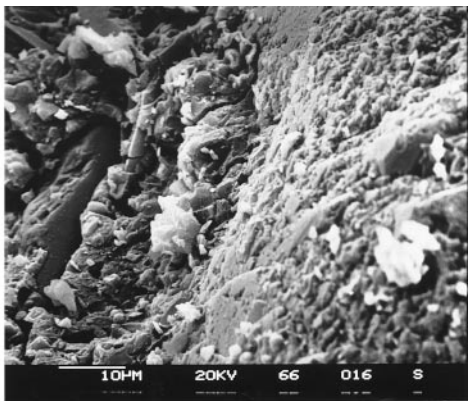
**Discussion**

**Microstructure of Interfacial Zone**

The SEM observation in this study confirms that a very porous transition zone, filled with well-formed  $\text{Ca}(\text{OH})_2$  crystals with c-axis parallel to the sand grain, exists between Portland cement paste and sand grain. However no porous zone is observed between the alkali-



(a)



(b)

FIG. 5.  
Transition zone between alkali-activated slag paste and sand.

activated slag paste and the sand grain. Another effective technique for interface investigation is the measurement of microhardness. It is well-known that the microhardness of the transition zone is much lower than that of bulk paste in Portland cement mortar or concrete. Several studies (19,20) have measured the microhardness of the transition zone between alkali-activated slag paste and different aggregates and no weak transition zone has been identified in the alkali-activated slag mortar, which will be explained later.

### **Interfacial Excess Conductance**

The interfacial excess conductance is the difference in electrical conductivity between interfacial zone and the bulk paste. The electrical conductivity of mortars depends not only on the pore structure, but also on the pore solution chemistry. Based on the SEM observation, no difference could be seen between the transition zone and the bulk paste in the alkali-activated slag mortars. However, several studies have confirmed that alkalis concentrate in the alkali-aggregate reaction rims around the reactive aggregate (20–21). Another study has found that alkalis can also concentrate in the transition zone around non-reactive aggregate (1). Thus, the positive interfacial excess conductance in the alkali-activated slag cement concrete may be due to the difference in the pore solution chemistry between the transition zone and the bulk pastes, instead of the difference in pore structure.

### **Interface Formation Mechanisms in Portland Cement Mortar and Concrete**

Several different hypothesis have been proposed to explain the formation of the transition zone between cement paste and aggregate in portland cement concrete:

- Formation of water layer on the non-porous aggregate surface at the beginning of the mixing of concrete mixture, inhibiting anhydrous grains from coming into contact with the interface.
- Flocculation of cement grains in contact with the aggregate, resulting in high local porosity.
- Inadequate intergrain filling due to wall effect, resulting in high local porosity.

Actually, no single model or mechanism can fully explain the formation of the porous transition zone between Portland cement paste and aggregate. The formation of the transition zone can be described as follows: When the cement paste is placed in contact with aggregate, a porous zone around aggregates forms due to the several reasons as described as above. The concentration difference between the transition zone and the rest of the paste leads to the migration of ions, such as  $\text{Na}^+$ ,  $\text{Ca}^{2+}$ ,  $\text{Al}^{3+}$  and  $\text{SO}_4^{2-}$ , during the hydration of cement and promotes  $\text{Ca}(\text{OH})_2$  and Aft growth in contact with the aggregates.

### **Hypothesis for the Interface Formation in Alkali-Activated Slag Mortars**

A more porous transition zone around quartz also forms as  $\text{Na}_2\text{SiO}_3$  activated slag pastes is placed in contact with sand grains due to the various effects as described as above. It is well known that sodium silicate is a water-reducing agent. It was visually observed during the mixing that  $\text{Na}_2\text{SiO}_3$ -activated slag pastes showed a higher workability than Portland cement



pastes for a given water to cement or slag ratio although no workability was measured. This means that  $\text{Na}_2\text{SiO}_3$  can reduce the flocculation of slag grains and the wall effect. Thus, it can be expected that the initial porous transition zone around quartz in  $\text{Na}_2\text{SiO}_3$ -activated slag mortars is smaller than that in Portland cement mortars.

The pore solution in  $\text{Na}_2\text{SiO}_3$ -activated slag has a very high concentration of  $[\text{SiO}_4]^{4-}$  (1.61 mol/L at the beginning in this study). The variation in  $\text{Ca}^{2+}$  concentration results in the migration of  $\text{Ca}^{2+}$  to the porous transition zone and the formation of C-S-H with a lower C/S ratio than that in the bulk paste, which fills pores around sand grains. As water is consumed due to the hydration of slag and electrolytes are released from the dissolution of slag grains, the excess  $[\text{SiO}_4]^{4-}$  in the solution will condense and act as an inorganic polymer in hardened mortars. It can be expected that no porous and weak interfacial zone will exist in  $\text{Na}_2\text{SiO}_3$ -activated slag mortars.

Sand grains have a very low dissolution rate and solubility in water. However, the dissolution rate and solubility will increase significantly with pH values greater than 12. The presence of alkalis also markedly increases the dissolution rate of quartz (22). The surface dissolution of sand grains will enhance the bonding between quartz and cement paste through two effects: formation of more products around sand grains and a rough surface that enhances mechanical interlock.

Some studies (10) have reported that the clays or silts on the surface of aggregate, which normally weaken the bond between Portland cement paste and aggregate, can react with the alkaline activator(s) to form cementitious compounds, however no sufficient evidences have been provided.

## Conclusions

This study has investigated the formation of microstructure of transition zone in  $\text{Na}_2\text{SiO}_3$ -activated slag mortars using electrical conductivity measurement, XRD analysis of hydration products and SEM observation. The following conclusions can be drawn based on the experimental results and analyses based on published results:

1. The measurement of electrical conductivity indicated that a positive interfacial conductance existed in  $\text{Na}_2\text{SiO}_3$ -activated slag mortars (or the electrical conductivity of the transition zone was higher than that of the bulk paste).
2. A very porous and weak transition zone was observed under SEM in Portland cement mortars, but a dense and uniform transition zone was observed in the  $\text{Na}_2\text{SiO}_3$ -activated slag mortars. The formation of the dense and uniform transition zone in the  $\text{Na}_2\text{SiO}_3$ -activated slag mortars can be attributed to several factors such as water reducing function of  $\text{Na}_2\text{SiO}_3$ , high initial concentration of  $[\text{SiO}_4]^{4-}$  in the pore solution and increased dissolution of quartz in such a high pH medium.
3. In Portland cement concrete, a positive interfacial excess conductance means the presence of a porous transition zone between cement paste and aggregate. An analysis based on literature review indicated that the positive interfacial excess conductance in alkali-activated slag cement concrete may be due to the difference in the pore solution chemistry between the transition zone and the bulk pastes, rather than the pore structure.

### References

1. D. Breton, A. Carles-Gibergues, G. Ballivy, and J. Grandet, *Cem. Concr. Res.* 23, 335–346 (1993).
2. J.C. Maso, *Proceedings of 7th International Congress on the Chemistry of Cements*, Vol. I, pp. VII - 1/4–1/15, Paris, 1980.
3. W. Sun, J.A. Mandel, and S. Said, *ACI J.* 83, 597–605, (1986).
4. P. Xie and J.J. Beaudoin, *Cem. Concr. Res.* 22, 597–604 (1992).
5. X. Wu, D. Li, and M. Tang, *Proceedings of Materials Research Society*, Vol. 114, pp. 35–40, 1988.
6. A. Bentur and M.D. Cohen, *J. Am. Ceram. Soc.* 70, 738–743 (1987).
7. M. Saito and M. Kawamura, *Proceedings of International Conference on the Fly Ash, Silica Fume, Slag and Natural Pozzolans in Concrete*, SP-114, American Concrete Institute, Vol. 1, pp. 669–688, 1989.
8. B. Talling and J. Bradstetr, *Proceedings of the 3rd International Conference on the Use of Fly Ash, Silica Fume, Slag & Natural Pozzolans in Concrete*, SP-114, pp. 1519–1546, Norway, June 1989.
9. C. Shi, R.L. Day, X. Wu, and M. Tang, *Proceedings of 9th International Congress on the Chemistry of Cements*, New Delhi, India, November, 1992.
10. P.V. Krivenko, *Proceedings of 1st International Conference on Alkaline Cements and Concretes*, Vol. 1, pp. 11–130, Kiev, 1994.
11. X. Pu, C. Gan, O. He, G. Bai, L. Wu, and M. Chen, *Proceedings of International Symposium on Concrete Engineering*, pp. 1144–1149, Nanjing, P. R. China, September, 1991.
12. P. Xie and M. Tang, *Il Cemento*, 85, 33–42 (1988).
13. P. Xie, J.J. Beaudoin, and R. Brousseau, *Cem. Concr. Res.* 21, 515–522 (1991).
14. P. Xie, J.J. Beaudoin, and R. Brousseau, *Cem. Concr. Res.* 21, 999–1005 (1991).
15. P. Xie, Ph.D Thesis, University of Ottawa, 1992.
16. C. Shi, *Cem. Concr. Res.*, in Press.
17. K. Mohan and H.F.W. Taylor, *Effects of Fly Ash Incorporation in Cement and Concrete*, S. Diamond (ed.), *Proceedings of MRS*, pp. 54–59, 1981.
18. Y. Deng, X. Wu, and M. Tang, *J. Nanjing Inst. Chem. Tech.* 11, 1–7 (1989).
19. V. P. Ilyin, *Proceedings of 1st International Conference on Alkaline Cements and Concretes*, Vol. 2, pp. 789–836, 1995.
20. H. Wang and J.E. Gillott, *Cem. Concr. Res.* 21, 647–654 (1991).
21. M. Brouxel, *Cem. Concr. Res.* 23, 309–320 (1993).
22. P.M. Dove and Rimstidt, *Silica-Water Interactions. Silica—Physical Behaviour, Geochemistry, and Materials Applications*, P.J. Heaney, C.T. Prewitt, and G.V. Gibbs (eds.), *Mineralogical Society of America*, Washington, D.C., 1995.